Adv. Geom. **10** (2010), 1–29
DOI 10.1515/ADVGEOM.2010.001

Advances in Geometry

Secant dimensions of low-dimensional homogeneous varieties

Karin Baur* and Jan Draisma†

(Communicated by R. Miranda)

Abstract. We completely describe the higher secant dimensions of all connected homogeneous projective varieties of dimension at most 3, in all possible equivariant embeddings. In particular, we calculate these dimensions for all Segre–Veronese embeddings of $\mathbb{P}^1 \times \mathbb{P}^1$, $\mathbb{P}^1 \times \mathbb{P}^1 \times \mathbb{P}^1$, and $\mathbb{P}^2 \times \mathbb{P}^1$, as well as for the flag variety $\mathcal{F}$ of incident point-line pairs in $\mathbb{P}^2$. For $\mathbb{P}^2 \times \mathbb{P}^1$ and $\mathcal{F}$ the results are new, while the proofs for the other two varieties are more compact than existing proofs. Our main tool is the second author's tropical approach to secant dimensions.

1 Introduction and results

Let K be an algebraically closed field of characteristic 0; all varieties appearing here will be over K. Let G be a connected affine algebraic group, and let X be a projective variety on which G acts transitively. An *equivariant embedding* of X is by definition a G-equivariant injective morphism $\iota : X \to \mathbb{P}(V)$, where V is a finite-dimensional (rational) G-module, subject to the additional constraint that $\iota(X)$ spans $\mathbb{P}(V)$.

The k-th (higher) secant variety $k\iota(X)$ of $\iota(X)$ is the closure in $\mathbb{P}(V)$ of the union of all subspaces of $\mathbb{P}(V)$ spanned by k points on $\iota(X)$. The *expected dimension* of $k\iota(X)$ is $\min\{k(\dim X + 1) - 1, \dim V - 1\}$; this is always an upper bound on $\dim k\iota(X)$. We call $k\iota(X)$ *non-defective* if it has the expected dimension, and *defective* otherwise. We call ι non-defective if $k\iota(X)$ is non-defective for all k, and defective otherwise.

We want to compute the secant dimensions of $\iota(X)$ for all X of dimension at most 3 and all ι. This statement really concerns only finitely many pairs (G, X): Indeed, as X is projective and G-homogeneous, the stabiliser of any point in X is parabolic (see [2, §11]) and therefore contains the solvable radical R of G. But then R also acts trivially on the span of $\iota(X)$, which is $\mathbb{P}(V)$, so that we may replace G by the quotient G/R, which is semisimple. In addition, we may and shall assume that G is simply connected. Now V is

*The first author is supported by EPSRC grant number GR/S35387/01.
†The second author is supported by DIAMANT, an NWO mathematics cluster.

an irreducible G-module, and $\iota(X)$ is the unique closed orbit of G in $\mathbb{P}V$, the cone over which in V is also known as the *cone of highest weight vectors*. Conversely, recall that for two dominant weights λ and λ' the minimal orbits in the corresponding projective spaces $\mathbb{P}V(\lambda)$ and $\mathbb{P}V(\lambda')$ are isomorphic (as G-varieties) if and only if λ and λ' have the same support on the basis of fundamental weights. So, to prove that all equivariant embeddings of a fixed X are non-degenerate, we have to consider all possible dominant weights with a fixed support.

Now there are precisely seven pairs (G, X) with $\dim X \leq 3$, namely $(\mathrm{SL}_2^i, (\mathbb{P}^1)^i)$ for $i = 1, 2, 3$, $(\mathrm{SL}_3, \mathbb{P}^2)$, $(\mathrm{SL}_3 \times \mathrm{SL}_2, \mathbb{P}^2 \times \mathbb{P}^1)$, $(\mathrm{SL}_4, \mathbb{P}^3)$, and $(\mathrm{SL}_3, \mathcal{F})$, where $\mathcal{F}$ is the variety of flags $p \subset l$ with p, l a point and a line in $\mathbb{P}^2$, respectively. The equivariant embeddings of $\mathbb{P}^i$ for $i = 1, 2, 3$ are the Veronese embeddings; their higher secant dimensions — and indeed, all higher secant dimensions of Veronese embeddings of projective spaces of arbitrary dimensions — are known from the work of Alexander and Hirschowitz; see [1] or [3]. In low dimensions there also exist tropical proofs for these results: $\mathbb{P}^1$ and $\mathbb{P}^2$ were given as examples in [10], and for $\mathbb{P}^3$ see the Master's thesis of Silvia Brannetti [4]. The other varieties are covered by the following theorems.

First, the equivariant embeddings of $\mathbb{P}^1 \times \mathbb{P}^1$ are the Segre–Veronese embeddings, parameterised by the degree (d, e) (corresponding to the highest weight $d\omega_1 + e\omega_2$ where the ω_i are the fundamental weights), where we may assume $d \geq e$. The following theorem is known in the literature; see for instance [5, Theorem 2.1] and the references there. Our proof is rather short and transparent, and serves as a good introduction to the more complicated proofs of the remaining theorems.

Theorem 1.1. *The Segre–Veronese embedding of $\mathbb{P}^1 \times \mathbb{P}^1$ of degree (d, e) with $d \geq e \geq 1$ is non-defective unless $e = 2$ and d is even, in which case the $(d+1)$-st secant variety has codimension 1 rather than the expected 0.*

The equivariant embeddings of $\mathbb{P}^1 \times \mathbb{P}^1 \times \mathbb{P}^1$ and of $\mathbb{P}^2 \times \mathbb{P}^1$ are also Segre–Veronese embeddings. While writing this paper we found out that the following theorem has already been proved in [6]. We include our proof because we need its building blocks for the other 3-dimensional varieties.

Theorem 1.2. *The Segre–Veronese embedding of $\mathbb{P}^1 \times \mathbb{P}^1 \times \mathbb{P}^1$ of degree (d, e, f) with $d \geq e \geq f \geq 1$ is non-defective unless*

(1) *$e = f = 1$ and d is even, in which case the $(d+1)$-st secant variety has codimension 1 rather than the expected 0, or*
(2) *$d = e = f = 2$, in which case the 7-th secant variety has codimension 1 instead of the expected 0.*

The remaining two theorems are newer.

Theorem 1.3. *The Segre–Veronese embedding of $\mathbb{P}^2 \times \mathbb{P}^1$ of degree (d, e) with $d, e \geq 1$ is non-defective unless*

(1) *$d = 2$ and $e = 2k$ is even, in which case the $(3k+1)$-st secant variety has codimension 3 rather than the expected 2 and the $(3k+2)$-nd secant variety has codimension 1 rather than 0; or*

(2) $d = 3$ *and* $e = 1$*, in which case the* 5*-th secant variety has codimension* 1 *rather than the expected* 0*.*

Finally, the equivariant embeddings of $\mathcal{F}$ are the minimal orbits in $\mathbb{P}V$ for any irreducible SL_3-representation of highest weight $d\omega_1 + e\omega_2$.

Theorem 1.4. *The image of* $\mathcal{F}$ *in* $\mathbb{P}V$*, for* V *an irreducible* SL_3*-representation of highest weight* $d\omega_1 + e\omega_2$ *with* $d, e \geq 1$ *is non-defective unless*

(1) $d = e = 1$*, in which case the* 2*-nd secant variety has codimension* 1 *rather than* 0*, or*
(2) $d = e = 2$*, in which case the* 7*-th secant variety has codimension* 1 *rather than* 0*.*

Remark 1.5. Most defective Segre–Veronese varieties above can be explained as follows. The Veronese varieties are rank-1 loci of so-called *catalecticant matrices*, whose entries are homogeneous coordinates of the ambient space [11]. The Segre product of such varieties is then the rank-1 locus of the Kronecker product of the corresponding catalecticant matrices. Hence the k-th secant variety of this Segre product is contained in the locus of rank-k matrices. In general this does not give much information about the ideal, but sometimes it is just enough to conclude that a secant variety that was expected to fill the space actually is contained in a hypersurface. This argument is used extensively in [7].

To the best of our knowledge Theorems 1.3 and 1.4 are new. Moreover, $\mathcal{F}$ seems to be the first settled case where maximal tori in G do not have dense orbits. Our proofs of Theorems 1.1 and 1.2 are more compact than their original proofs [5, 6]. Moreover, the planar proof of Theorem 1.1 serves as a good introduction to the more complicated induction in the three-dimensional cases, while parts of the proof of Theorem 1.2 are used as building blocks in the remaining proofs.

We shall prove our theorems using a polyhedral-combinatorial lower bound on higher secant dimensions introduced by the second author in [10]. Roughly this goes as follows: to a given X and V we associate a finite set B of points in $\mathbb{R}^{\dim X}$, which parameterises a certain basis in V. Now to find a lower bound on $\dim kX$ we *maximise*

$$\sum_{i=1}^{k} [1 + \dim \mathrm{Aff}_{\mathbb{R}} \mathrm{Win}_i(f)]$$

over all k-tuples $f = (f_1, \ldots, f_n)$ of affine-linear functions on $\mathbb{R}^{\dim X}$, where $\mathrm{Win}_i(f)$ is the set of points in B where f_i is strictly smaller than all f_j with $j \neq i$, and where $\mathrm{Aff}_{\mathbb{R}}$ denotes taking the affine span. Typically, this maximum equals 1 plus the expected dimension of $\dim k\iota(X)$, and then we are done. If not, then we need other methods to prove that $k\iota(X)$ is indeed defective — but most defective cases above are known in the literature.

As a motivation for this optimisation problem we now carry out our proof in one particular case. For the Segre–Veronese embedding of $X = \mathbb{P}^1 \times \mathbb{P}^1$ of degree (d, e) the set B is the grid $\{0, \ldots, d\} \times \{0, \ldots, e\} \subseteq \mathbb{R}^2$. Take for instance $d = 3$ and $e = 2$. In Figure 1 the points in B are grouped into four triples spanning the plane. It is easy to see — for instance with Lemma 2.6 below — that there exist affine-linear functions $f_1, \ldots, f_4$ inducing this partition, so that $4X$ has the expected dimension $4 \cdot 3 - 1 = 11$.

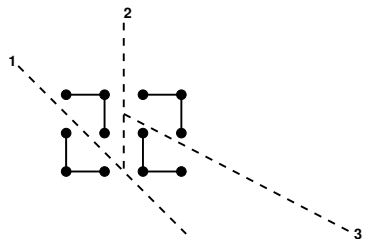

Figure 1: The embedding $\mathrm{Seg} \circ (v_3 \times v_2)$ of $\mathbb{P}^1 \times \mathbb{P}^1$ is non-defective.

Our tropical approach closely related to Sturmfels–Sullivant's combinatorial secant varieties [13], Miranda–Dumitrescu's degeneration approach (private communication), and Develin's tropical secant varieties of linear spaces [9]. We find it very surprising and promising that strong results on secant varieties of non-toric varieties such as $\mathcal{F}$ can be proved with our approach.

The remainder of this paper is organised as follows. In Section 2 we recall the tropical approach, and prove a lemma that will help us deal with the flag variety. The tropical approach depends rather heavily on a parameterisation of X, and in Section 3 we introduce the polynomial maps that we shall use. In particular, we give, for any minimal orbit (not necessarily of low dimension, and not necessarily toric), a polynomial paramaterisation whose tropicalisation has an image of the right dimension; these tropical parameterisations are useful in studying tropicalisations of minimal orbits; see Remark 3.3. Finally, Sections 4–7 contain the proofs of Theorems 1.1–1.4, respectively.

Acknowledgments. We thank the referee for such thorough reading of the first version of this paper, and for many suggestions to improve it.

2 The tropical approach

2.1 Two optimisation problems. We recall from [10] a polyhedral-combinatorial optimisation problem that plays a crucial role in the proofs of our theorems; here AP abbreviates *Affine Partition*.

Problem 2.1 ($\mathrm{AP}(A,k)$). Let $A = (A_1, \ldots, A_n)$ be a sequence of finite subsets of $\mathbb{R}^m$ and let $k \in \mathbb{N}$. For any k-tuple $f = (f_1, \ldots, f_k)$ of affine-linear functions on $\mathbb{R}^m$ let the sets $\mathrm{Win}_i(f)$, $i = 1, \ldots, k$, be defined as follows. For $b = 1, \ldots, n$ we say that f_i *wins* b if f_i attains its minimum on A_b in a unique $\alpha \in A_b$, and if this minimum is strictly smaller than all values of all $f_j, j \neq i$ on A_b. The vector α is then called a *winning direction* of f_i. Let $\mathrm{Win}_i(f)$ denote the set of winning directions of f_i. Now the problem $\mathrm{AP}(A,k)$ can be stated as follows.

Maximise $\sum_{i=1}^{k} [1 + \dim \mathrm{Aff}_{\mathbb{R}} \mathrm{Win}_i(f)]$ *over all k-tuples f of affine-linear functions on $\mathbb{R}^m$; call the maximum* $\mathrm{AP}^*(A,k)$.

Note that if every A_b is a singleton $\{\alpha_b\}$, then $\mathrm{Win}_i(f)$ is just the set of all α_b on which f_i is smaller than all other $f_j, j \neq i$. We shall then also write $\mathrm{AP}(\{\alpha_1, \ldots, \alpha_n\}, k)$ for the optimisation problem above. In this case we are really optimising over all possible *regular subdivisions* of $\mathbb{R}^m$ into k open cells. Each such subdivision induces a partition of the α_b into the sets $\mathrm{Win}_i(f)$ — at least if no α_b lies on a border between two cells, but this is easy to achieve without decreasing the objective function. Below we shall never explicitly construct the f_j, nor the regular subdivision, but rather just give the induced partition on the points α_i, which will lie in two- or three-dimensional real space depending on the dimension of X. The following two lemmas will be used throughout to establish the existence of the f_i without actually constructing them.

Lemma 2.2. *Let S be a finite set in $\mathbb{R}^m$, let $f_1, \ldots, f_k$ be affine-linear functions on $\mathbb{R}^m$, and let $g_1, \ldots, g_l$ also be affine-linear functions on $\mathbb{R}^m$. Let S_i be the subset of S where $f_i < f_j$ for all $j \neq i$, and let T_i be the subset of S_1 where $g_i < g_j$ for all $j \neq i$. Then there exist affine-linear functions $h_1, \ldots, h_l$ such that*

(1) *$h_i < h_j$ on T_i for $i, j = 1, \ldots, l$ and $j \neq i$;*
(2) *$h_i < f_j$ on T_i for $i = 1, \ldots, l$ and $j = 2, \ldots, k$; and*
(3) *$f_i < h_j$ on S_i for $i = 2, \ldots, k$ and $j = 1, \ldots, l$.*

In other words, the functions $h_1, \ldots, h_l, f_2, \ldots, f_k$ together induce the partition $T_1, \ldots, T_l, S_2, \ldots, S_k$ of S.

Proof. Take $h_i = f_1 + \varepsilon g_i$ for ε positive and sufficiently small. □

This lemma implies, for instance, that one may find appropriate $\mathrm{Win}_i(f)$ (still for the case of singletons A_b) by repeatedly cutting polyhedral pieces of space in half. For instance, in Figure 1 the plane is cut into four pieces by three straight cuts. Although this is not a regular subdivision of the plane, by the lemma there does exist a regular subdivision of the plane inducing the same partition on the 12 points. The next lemma concerns the following, slightly different polyhedral optimisation problem *Voronoi Partition*.

Problem 2.3 ($\mathrm{VP}(S, k)$). Let S be a finite set in $\mathbb{R}^m$, and equip $\mathbb{R}^m$ with a positive definite inner product with associated norm $||\ .\ ||$. For any k-tuple $v = (v_1, \ldots, v_k)$ of points in $\mathbb{R}^m$ let $\mathrm{Vor}_i(v)$ denote the intersection of S with the open Voronoi cell of v_i, i.e.,

$$\mathrm{Vor}_i(v) := \{\alpha \in S \mid ||\alpha - v_i|| < ||\alpha - v_j|| \text{ for all } j \neq i\}.$$

Then the problem $\mathrm{VP}(S, k)$ can be stated as follows.

Maximise $\sum_{i=1}^{k} [1 + \dim \mathrm{Aff}_{\mathbb{R}} \mathrm{Vor}_i(v)]$ *over all k-tuples v of points in $\mathbb{R}^m$; call the maximum* $\mathrm{VP}^*(A, k)$.

Lemma 2.4 ([10, Lemma 3.8]). *Let S be a finite subset in the Euclidean space $(\mathbb{R}^m, ||\ .\ ||)$, let $v = (v_1, \ldots, v_k)$ be a k-tuple of points in $\mathbb{R}^m$ for which the sets $\mathrm{Vor}_i(v)$ partition S, that is, there are no points of S on the boundary of any Voronoi cell. Then there exists a k-tuple $f = (f_1, \ldots, f_k)$ of affine-linear functions on $\mathbb{R}^m$ whose associated regular subdivision partitions the set S in exactly the same parts $\mathrm{Vor}_i(S)$. In particular, $\mathrm{AP}^*(S, k) \leq \mathrm{VP}^*(S, k)$.*

Lemmas 2.2 and 2.4 can only be applied directly to AP if the A_b are singletons, while the A_b in our application to the 3-dimensional flag variety $\mathcal{F}$ are not. We get around this difficulty by giving a lower bound on $\mathrm{AP}^*(A,k)$ for more general A in terms of $\mathrm{AP}^*(A',k)$ for some sequence A' of singletons. In the following lemmas a *convex polyhedral cone* in $\mathbb{R}^m$ is by definition the set of non-negative linear combinations of a finite set in $\mathbb{R}^m$, and it is called *pointed* if it does not contain any non-trivial linear subspace of $\mathbb{R}^m$.

Lemma 2.5. *Let $A = (\{\alpha_1\},\ldots,\{\alpha_n\})$ be an n-tuple of singleton subsets of $\mathbb{R}^m$. Furthermore, let $k \in \mathbb{N}$, let Z be a pointed convex polyhedral cone in $\mathbb{R}^m$, and let f be a k-tuple of affine-linear functions on $\mathbb{R}^m$. Then the value of $\mathrm{AP}(A,k)$ at f is also attained at some $f' = (f'_1,\ldots,f'_k)$ for which every f'_i is strictly decreasing in the z-direction, for every $z \in Z \setminus \{0\}$.*

Proof. As Z is pointed, there exists a linear function f_0 on $\mathbb{R}^m$ such that every $f_j + f_0$ is strictly decreasing in the z-direction, for every $z \in Z$. But since

$$f_i(\alpha) < f_j(\alpha) \Leftrightarrow f_i(\alpha) + f_0(\alpha) < f_j(\alpha) + f_0(\alpha)$$

we have $\mathrm{Win}_i((f_j + f_0)_j) = \mathrm{Win}_i(f)$ for all i, and we are done. □

It is crucial in this proof that only values of f_i and f_j at *the same* α are compared — that is why we have restricted ourselves to singleton-AP here.

Lemma 2.6. *Let $A = (A_1,\ldots,A_n)$ be a k-tuple of finite subsets of $\mathbb{R}^m$ and let $k \in \mathbb{N}$. Furthermore, let Z be a pointed convex polyhedral cone in $\mathbb{R}^m$ and define a partial order $\leq$ on $\mathbb{R}^m$ by*

$$p \leq q :\Leftrightarrow p - q \in Z.$$

Suppose that for every b, A_b has a unique minimal element α_b with respect to this order. Then we have

$$\mathrm{AP}^*(A,k) \geq \mathrm{AP}^*(\{\alpha_1,\ldots,\alpha_n\},k)$$

Proof. Let $d^* = \mathrm{AP}^*(\{\alpha_1,\ldots,\alpha_n\},k)$. By Lemma 2.5 there exists a k-tuple $f = (f_1,\ldots,f_k)$ of affine-linear functions on $\mathbb{R}^m$ for which $\mathrm{AP}(\{\alpha_1,\ldots,\alpha_n\},k)$ also has value d^* and for which every f_i is strictly decreasing in all directions in Z. We claim that the value of $\mathrm{AP}(A,k)$ at this f is also d^*. Indeed, fix $b \in B$ and consider all $f_i(\alpha)$ with $\alpha \in A_b$ and $i = 1,\ldots,k$. Because $\alpha_b - \alpha \in Z$ for all $\alpha \in A_b$ and because every f_i is strictly decreasing in the directions in Z, we have $f_i(\alpha_b) < f_i(\alpha)$ for all $\alpha \in A_b \setminus \{\alpha_b\}$ and all i. Hence the minimum, over all pairs $(i,\alpha) \in \{1,\ldots,k\} \times A_b$, of $f_i(\alpha)$ can only be attained in pairs for which $\alpha = \alpha_b$. Therefore, in computing the value at f of $\mathrm{AP}(A,k)$ the elements of A_b unequal to α_b can be ignored. We conclude that $\mathrm{AP}(A,k)$ has value d^* at f, as claimed. This shows the inequality. □

2.2 Tropical bounds on secant dimensions. Rather than working with projective varieties, we work with the affine cones over them. So suppose that $C \subseteq K^n$ is a closed cone (i.e., closed under scalar multiplication with K), and set

$$kC := \overline{\{v_1 + \cdots + v_k \mid v_1, \ldots, v_k \in C\}}.$$

Suppose that C is unirational, and choose a polynomial map $f = (f_1, \ldots, f_n) : K^m \to C \subseteq K^n$ that maps K^m dominantly into C. Let $x = (x_i)_{i=1}^m$ and $y = (y_b)_{b=1}^n$ be the standard coordinates on K^m and K^n. The tropical approach depends very much on these coordinates; in particular, one would like f to be sparse. For every $b = 1, \ldots, n$ let A_b be the set of $\alpha \in \mathbb{N}^m$ for which the monomial x^α has a non-zero coefficient in f_b, and set $A := (A_1, \ldots, A_n)$.

Theorem 2.7 ([10]). *For all $k \in \mathbb{N}$, $\dim kC \geq \mathrm{AP}^*(A, k)$.*

Remark 2.8. In fact, in [10] this is proved provided that $\bigcup_b A_b$ is contained in an affine hyperplane not through 0, but this can always be achieved by taking a new map $f'(t, x) := tf(x)$ into C, without changing the optimisation problem $\mathrm{AP}(A, k)$.

In Section 3 we introduce a polynomial map f for general minimal orbits that seems suitable for the tropical approach, and after that we specialise to low-dimensional varieties under consideration.

2.3 Non-defective pictures. Our proofs will be entirely pictorial: given a set B of lattice points in $\mathbb{Z}^2$ or $\mathbb{Z}^3$ according as $\dim X = 2$ or $\dim X = 3$, we solve the optimisation problem $\mathrm{AP}(B, k)$ for all k. To this end, we shall exhibit a partition of B into parts B_i such that there exist affine-linear functions f_i on $\mathbb{R}^2$ or $\mathbb{R}^3$, exactly one for each part, with $B_i = \mathrm{Win}_i(f)$. If each B_i is affinely independent, and if moreover the affine span of each B_i has $\dim X$, except possibly for one single B_i, then we call the picture *non-defective*, as it shows, by Theorem 2.7, that all secant varieties of X in the given embedding have the expected dimension. Otherwise, we call the picture *defective*.

The B_i that we shall use will have very simple shapes: in dimension 2 they will all be equivalent, up to distance-preserving automorphisms of the lattice $\mathbb{Z}^2$, to the triple $\{0, e_1, e_2\}$, or to the edge $\{0, e_1\}$, or to the single point $\{0\}$. These building blocks also appear in dimension 3, but there we also have 3-dimensional blocks equivalent to $\{0, e_1, e_2, e_3\}$, which we call *corners*, or to $\{0, e_1, e_1 + e_2, e_1 + e_2 + e_3\}$, which we call *snakes*; see Figure 2. Only for the flag-variety $\mathcal{F}$ it will be convenient to use a single slightly different building block in one instance.

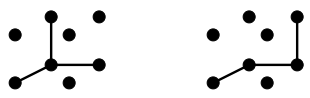

Figure 2: A corner (left) and a snake (right).

The f_i will not be computed explicitly, but their existence will be deduced from Lemmas 2.4 and 2.2 as follows. As a first approximation, to establish a Voronoi subdivision

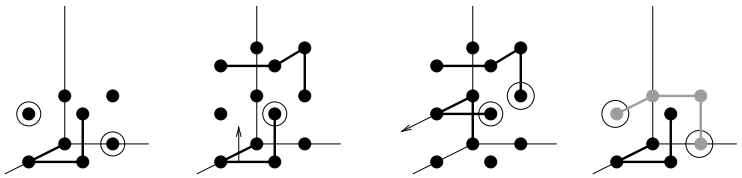

Figure 3: Snakes and threats

inducing the given partition of B into the B_i, one can try and take the barycentre M_i of each B_i as its point v_i. The squared distance, relative to the standard inner product, of this barycentre of B_i to its vertices is as follows:

single point $\{0\}$**:** 0;
edge $\{0, e_1\}$**:** twice $1/4$;
triangle $\{0, e_1, e_2\}$**:** once $2/9$, twice $5/9$;
corner $\{0, e_1, e_2, e_3\}$**:** once $3/16$, thrice $11/16$; and
snake $\{0, e_1, e_1 + e_2, e_1 + e_2 + e_3\}$**:** twice $6/16$, twice $14/16$ (for the *heads* of the snake).

Given any snake B_j, there are exactly two lattice points outside B_j that also have squared distance $14/16$ from the barycentre M_j. They are indicated with a circle in the left-most picture in Figure 3. If such a point p happens to be the head of another snake B_i, then we say that p is *threatened* by B_j, as it lies on the border of the Voronoi cells of B_i and B_j. It can happen that both B_j threatens a head of B_i, and B_i threatens a head of B_j; see the third picture in Figure 3 for an example. It is straightforward to verify that if all blocks B_i are of the shapes above, then any lattice point p of B_i is closer to M_i than to any M_j with $j \neq i$ *unless* p is threatened by B_j in the sense above. In our pictures we will then draw a circle around p, to indicate that it is threatened by B_j. Now our pictures are constructed in such a way that all such threats can be removed by slightly wiggling the v_i from their initial positions M_i. For snake B_j threatening the head p of snake B_i this can be done in more than one way: either by moving v_i from M_i slightly towards p, or by moving v_j from M_j slightly away from p. In our pictures we indicate such wigglings with small arrows: an arrow attached to (the edges connecting) B_i indicates that v_i is moved slightly in the direction of the arrow; see the second picture in Figure 3. This wiggling direction will always be one of the six positive or negative coordinate directions.

Remark 2.9. It is admittedly somewhat cumbersome to verify that the indicated wigglings do indeed remove all threats. It would be nicer to have a theorem stating that any partition of a point set B in $\mathbb{Z}^3$ into single points, edges, triangles, corners, and snakes is induced by some regular subdivision. However, this naive statement is not true for the simple reason that the two snakes in the rightmost picture in Figure 3 cannot be separated by a hyperplane. Now of course two such snakes can be replaced by two corners, and it might be true that any partition of B avoiding two such snakes is induced by some regular subdivision. However, we did not manage to prove anything substantial along these lines. Instead we have tried to reduce the number of threats in our pictures so that the reader can verify the pictorial proof with the following straightforward visual check: for each snake,

look at each of the two vertices that it potentially threatens. If that is the head of an other snake, one or both of the snakes should have arrows removing this threat.

In our proofs by induction we shall build non-defective pictures for sets B using non-defective pictures for smaller sets built earlier. To ensure that the resulting partition of B is indeed induced by some regular subdivision, one can proceed in two ways. First, if the smaller pictures can be separated by each other by a regular subdivision, e.g. by repeatedly cutting with planar cuts, then we may invoke Lemma 2.2. Occasionally, however, we shall match up redundant points from two smaller pictures to form a new building block (snake, corner, etc.). In such a situation we invoke Lemma 2.4, after checking that potential new threats created near the building block are removed by wiggling as above.

3 A polynomial map

We retain the setting of the Introduction: G is a simply connected, connected, semisimple algebraic group, V is a G-module, and we wish to determine the secant dimensions of X, the unique closed orbit of G in $\mathbb{P}V$. Let C be the affine cone in V over X. Fix a Borel subgroup B of G, let T be a maximal torus of B and let $v_\lambda \in V$ span the unique B-stable one-dimensional subspace of V; λ denotes the T-weight of v_λ. In other words, v_λ is a highest weight vector and λ is the highest weight of V. Let $P \supseteq B$ be the stabiliser in G of Kv_λ (so that $X \cong G/P$ as a G-variety) and let U_- be the unipotent radical of the parabolic subgroup opposite to P and containing T. Let $\mathfrak{u}$ denote the Lie algebra of U_-, let $X(\mathfrak{u})$ be the set of T-roots on $\mathfrak{u}$, and set $\tilde{X}(\mathfrak{u}) := X(\mathfrak{u}) \cup \{0\}$. For every $\beta \in X(\mathfrak{u})$ choose a vector X_β spanning the root space $\mathfrak{u}_\beta$. Moreover, fix an order on $X(\mathfrak{u})$. Then it is well known that the polynomial map

$$\Psi : K^{\tilde{X}(\mathfrak{u})} \to V,\ t \mapsto t_0 \prod_{\beta \in X(\mathfrak{u})} \exp(t_\beta X_\beta) v_\lambda,$$

where the product is taken in the fixed order, maps dominantly into C. This map will play the role of f from Subsection 2.2.

In what follows we shall need the following notation: Let $X_\mathbb{R} := \mathbb{R} \otimes_\mathbb{Z} X(T)$ be the real vector space spanned by the character group of T, let $\xi : \mathbb{R}^{X(\mathfrak{u})} \mapsto X_\mathbb{R}$ send r to $\sum_\beta r_\beta \beta$ and also use ξ for the map $\mathbb{R}^{\tilde{X}(\mathfrak{u})} \to X_\mathbb{R}$ with the same definition; in both cases we call $\xi(r)$ the *weight* of r.

Now for a basis of V: since V is a G-module with P stabilizing the line Kv_λ through the highest weight vector, all of V is obtained by letting the universal enveloping algebra of $\mathfrak{u}$ act on v_λ. The Poincaré–Birkhoff–Witt (PBW) theorem tells us that for any linear order on the basis $(X_\beta)_{\beta \in X(\mathfrak{u})}$ of $\mathfrak{u}$, the universal enveloping algebra of $\mathfrak{u}$ has a basis $\{\prod_{\beta \in X(\mathfrak{u})} X_\beta^{r_\beta} \mid r_\beta \in \mathbb{N}^{X(\mathfrak{u})}\}$, where the product is taken in the fixed order; cf. Section 17 of [12]. As a consequence, V is the linear span of the elements obtained by letting this basis act on v_λ, that is, of all elements of the form $m_r := \prod_{\beta \in X(\mathfrak{u})} X_\beta^{r_\beta} v_\lambda$ with $r \in \mathbb{N}^{X(\mathfrak{u})}$. Note that only finitely many of these are non-zero since each $X_\beta, \beta \in X(\mathfrak{u})$ acts nilpotently on V. Slightly inaccurately, we shall call the m_r PBW-monomials. Note that the T-weight of m_r is $\lambda + \xi(r)$.

Let M be the subset of all $r \in \mathbb{N}^{X(\mathfrak{u})}$ for which m_r is non-zero; M is finite. Let B be a subset of M such that $\{m_r \mid r \in B\}$ is a basis of V; later on we shall add further restrictions on B. For $b \in B$ let Ψ_b be the component of Ψ corresponding to b; it equals t_0 times a polynomial in the $t_\beta,\ \beta \in X(\mathfrak{u})$. Let $A_b \subseteq \mathbb{N}^{X(\mathfrak{u})}$ denote the set of exponent vectors of monomials having a non-zero coefficient in Ψ_b/t_0.

Lemma 3.1. *For $b_0 \in B$ we have*

(1) $A_{b_0} \subseteq \{r \in M \mid \xi(r) = \xi(b_0)\}$, *and*
(2) $A_{b_0} \cap B = \{b_0\}$.

Proof. Expand $\Psi(t)/t_0$ as a linear combination of PBW-monomials:

$$\Psi(t)/t_0 = \sum_{r \in \mathbb{N}^{X(\mathfrak{u})}} \frac{t^r}{\prod_{\beta \in X(\mathfrak{u})}(r_\beta!)} m_r.$$

So t^r appears in Ψ_{b_0}/t_0 if and only if m_r has a non-zero m_{b_0}-coefficient relative to the basis $(m_b)_{b \in B}$. Hence the first statement follows from the fact that every m_r is a linear combination of the m_b of the same T-weight as m_r, and the second statement reflects the fact that for all $b_1 \in B$, m_{b_1} has precisely one non-zero coefficient relative to the basis $(m_b)_{b \in B}$, namely that of m_{b_1}. □

Now Theorem 2.7 implies the following proposition.

Proposition 3.2. $\dim kC \geq \mathrm{AP}^*((A_b)_{b \in B}, k)$

For Segre products of Veronese embeddings every A_b is a singleton, and we can use our hyperplane-cutting procedure immediately. For the flag variety $\mathcal{F}$ we shall use Lemma 2.6 to bound AP^* by a singleton-AP^*.

Remark 3.3. To see that Proposition 3.2 has a chance of being useful, it is instructive to verify that $\mathrm{AP}^*((A_b)_{b \in B}, 1)$ is, indeed, $\dim C$, at least for some choices of B. Indeed, recall that the $|X(\mathfrak{u})| + 1$ vectors v_λ and $X_\beta v_\lambda$, $\beta \in X(\mathfrak{u})$, are linearly independent, so that we can take B to contain the corresponding exponent vectors, that is, 0 and the standard basis vectors e_β in $\mathbb{N}^{X(\mathfrak{u})}$. Now let $f_1 : \mathbb{R}^{X(\mathfrak{u})} \to \mathbb{R}$ send r to $\sum_{\beta \in X(\mathfrak{u})} r_\beta$. We claim that $\mathrm{AP}((A_b)_{b \in B}, k)$ has value $\dim C$ at (f_1). Indeed, $A_0 = \{0\}$ and for every $b \in B$ of the form e_β, $\beta \in X(\mathfrak{u})$, the set A_b consists of e_β itself, with f_1-value 1, and exponent vectors having a f_1-value a natural number > 1. Hence $\mathrm{Win}_1(f_1)$ contains all e_β and 0 — and therefore spans an affine space of dimension $\dim C - 1 = \dim X$.

This observation is of some independent interest for tropical geometry: going through the theory in [10], it shows that the image of the tropicalisation of Ψ in the tropicalisation of C has the right dimension; this is useful in minimal orbits such as Grassmannians.

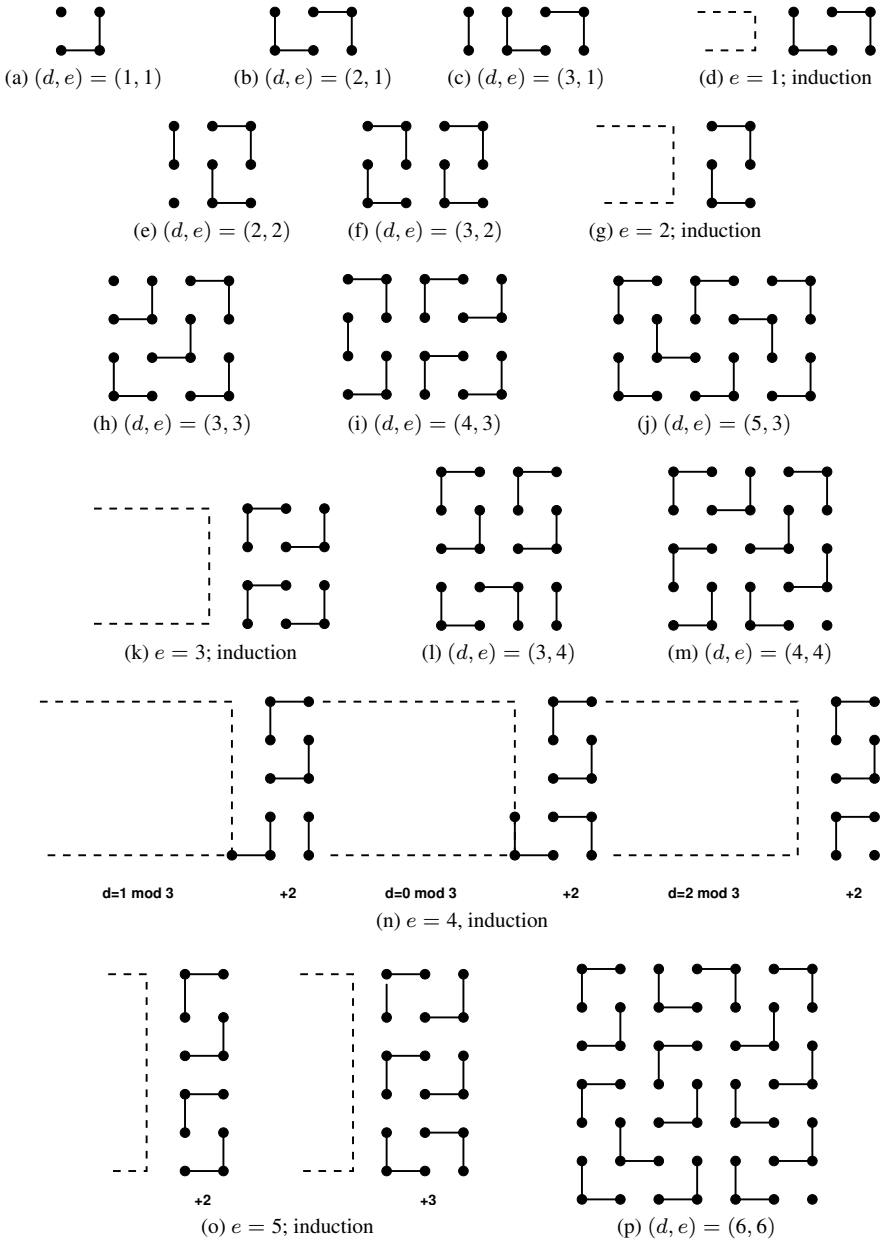

(a) $(d,e)=(1,1)$ (b) $(d,e)=(2,1)$ (c) $(d,e)=(3,1)$ (d) $e=1$; induction

(e) $(d,e)=(2,2)$ (f) $(d,e)=(3,2)$ (g) $e=2$; induction

(h) $(d,e)=(3,3)$ (i) $(d,e)=(4,3)$ (j) $(d,e)=(5,3)$

(k) $e=3$; induction (l) $(d,e)=(3,4)$ (m) $(d,e)=(4,4)$

(n) $e=4$, induction

(o) $e=5$; induction (p) $(d,e)=(6,6)$

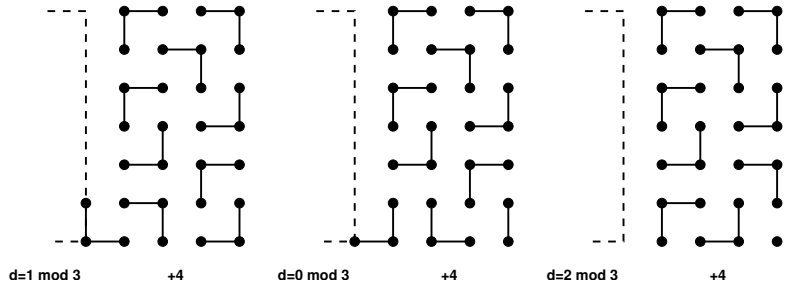

(q) $e = 6$; induction

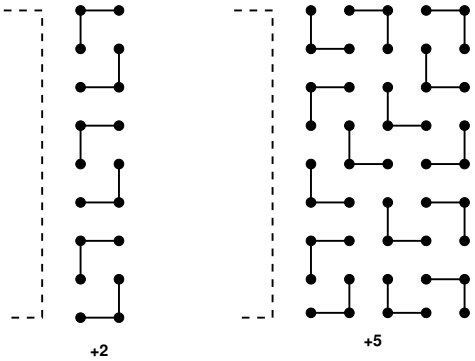

(r) $e = 8$; induction

Figure 4: More non-defective pictures for $\mathbb{P}^1 \times \mathbb{P}^1$.

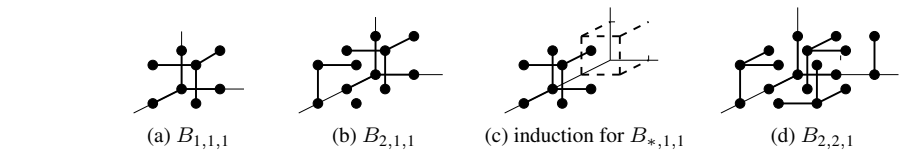

(a) $B_{1,1,1}$ (b) $B_{2,1,1}$ (c) induction for $B_{*,1,1}$ (d) $B_{2,2,1}$

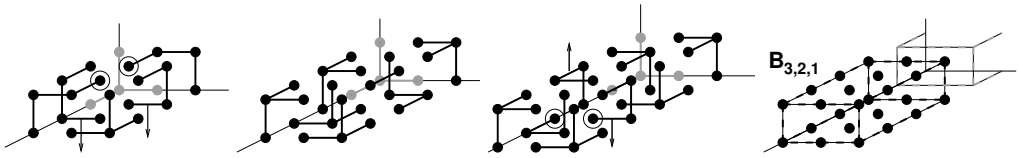

(e) $B_{3,2,1}$ (f) $B_{4,2,1}$ (g) $B_{5,2,1}$ (h) induction for $B_{*,2,1}$

Figure 5: Non-defective pictures for $(e, f) = (1, 1)$ or $(2, 1)$

4 Secant dimensions of $\mathbb{P}^1 \times \mathbb{P}^1$

We retain the notation of Section 3. To prove Theorem 1.1, let $X = \mathbb{P}^1 \times \mathbb{P}^1$, $G = \mathrm{SL}_2 \times \mathrm{SL}_2$, and $V = S^d(K^2) \otimes S^e(K^2)$. The polynomial map

$$\Psi : (t_0, t_1, t_2) \mapsto t_0(x_1 + t_1x_2)^d \otimes (x_1 + t_2x_2)^e,$$

is dominant into the cone C over X, and $M = B$ is the rectangular grid $\{0, \dots, d\} \times \{0, \dots, e\}$. We may assume that $d \geq e$. The building blocks of our non-defective pictures will be equivalent to $\{0\}, \{0, e_1\}$, or $\{0, e_1, e_2\}$. In particular, Lemma 2.4 can be applied directly to the barycentres of these blocks — there are no snakes and no threats.

First, if $e = 2$ and d is even, then $(d+1)C$ is known to be defective, that is, it does not fill V but is given by some determinantal equation; see [7, Example 3.2]. The argument below will show that its defect is not more than 1.

Figure 4 gives non-defective pictures for $e = 1, 2, 3, 4, 5$ and $d \geq e$, except for $e = 2$ and d even. This implies, by transposing pictures, that there exist non-defective pictures for $e = 6$ and $d = 1, 3, 4, 5$. Figure 4p gives a non-defective picture for $(d, e) = (6, 6)$. Then, using the two induction steps in Figure 4q, we find non-defective pictures for $e = 6$ and all $d \neq 2$. A similar reasoning gives non-defective pictures for $e = 8$ and all $d \neq 2$. Finally, let $d \geq e \geq 6$ be arbitrary with $(d, e) \notin 2\mathbb{N} \times \{2\}$. Write $e + 1 = 6q + r$ with $r \in \{0, 2, 4, 5, 7, 9\}$. Then we find a non-defective picture for (d, e) by gluing q non-defective pictures for $(d, 5)$ and, if $r \neq 0$, one non-defective picture for $(d, r - 1)$ on top of each other. This proves Theorem 1.1.

5 Secant dimensions of $\mathbb{P}^1 \times \mathbb{P}^1 \times \mathbb{P}^1$

Now we turn to Theorem 1.2. Cutting to the chase, $M = B$ is the block $\{0, \dots, d\} \times \{0, \dots, e\} \times \{0, \dots, f\}$. We denote the picture for this block by $B_{d,e,f}$. When convenient we assume that $d \geq e \geq f$. First, for $e = f = 1$ and d even, the $d + 1$-st secant variety, which one would expect to fill the space, is in fact known to be defective, see [6]. The pictures below show that the defect is not more than 1.

Figure 5 gives inductive constructions for pictures for $(e, f) \in \{(1, 1), (2, 1)\}$ that are non-defective except for $(e, f) = (1, 1)$ and d even. The grey shades serve no other purpose than to distinguish between front and behind.

Rotating appropriately, this also gives non-defective pictures $B_{1,3,1}$ and $B_{2,3,1}$; Figure 6b then gives an inductive construction of non-defective pictures $B_{d,3,1}$ for $d \geq 3$.

So far we have found non-defective pictures $B_{2,4,1}$ and $B_{3,4,1}$ (just rotate those $B_{4,2,1}$ and $B_{4,3,1}$). Figure 6c gives a non-defective picture $B_{4,4,1}$. A non-defective picture $B_{5,4,1}$ can be constructed from a $B_{5,1,1}$ and $B_{5,2,1}$. Now let $d \geq 6$ and write $d + 1 = 4q + r$ with $q \geq 0$ and $r \in \{3, 4, 5, 6\}$. Then using q copies of $B_{3,4,1}$ and 1 copy of $B_{r-1,4,1}$, we can build a non-defective picture $B_{d,4,1}$; see Figure 6d for this inductive procedure.

We already have non-defective pictures $B_{1,5,1}$ and $B_{2,5,1}$. For $d \geq 3$, write $d + 1 = q * 2 + r$ with $r \in \{2, 3\}$. Then a non-defective picture $B_{d,5,1}$ can be constructed from q copies of our non-defective picture $B_{1,5,1}$ and 1 copy of our non-defective picture $B_{r-1,5,1}$.

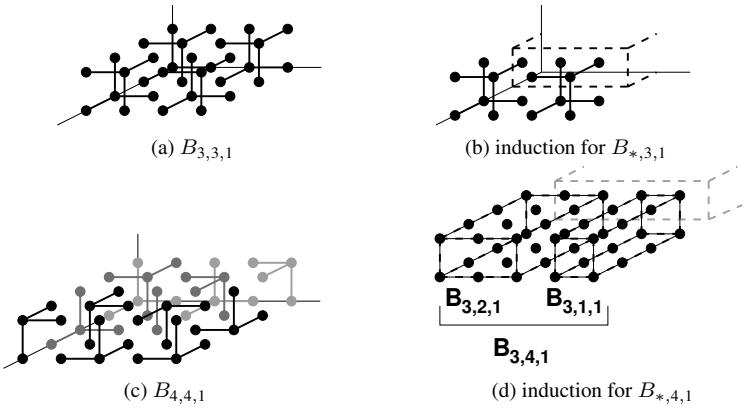

(a) $B_{3,3,1}$ (b) induction for $B_{*,3,1}$

(c) $B_{4,4,1}$ (d) induction for $B_{*,4,1}$

Figure 6: Non-defective pictures for $B_{*,3,1}$ and $B_{*,4,1}$.

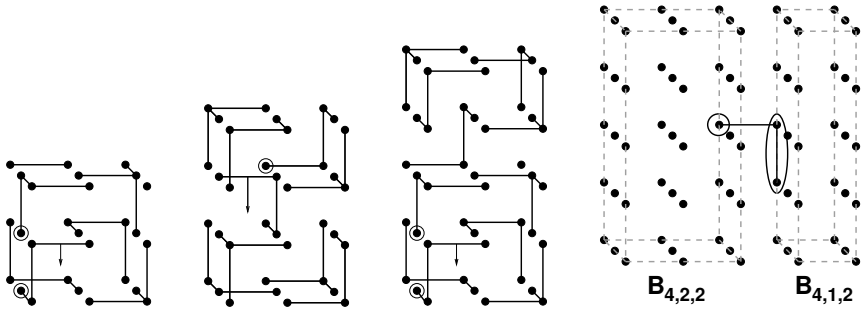

(a) $B_{2,2,2}$ (b) $B_{3,2,2}$ (c) $B_{4,2,2}$ (d) $B_{4,4,2}$

Figure 7: Non-defective pictures for some $B_{*,*,2}$.

Let $d \geq e \geq 6$ and write $e+1 = q*4+r$ with $r \in \{3,4,5,6\}$. Then we can construct a non-defective picture $B_{d,e,1}$ by putting together q non-defective pictures $B_{d,3,1}$ and 1 non-defective picture $B_{d,r-1,1}$. This settles all cases of the form $B_{d,e,1}$.

Figure 7a gives a picture for $(d,e,f) = (2,2,2)$, The picture is defective, but it shows that kX has the expected dimension for $k = 1,\ldots,6$ and defect at most 1 for $k = 7$. From [6] we know that $7X$ is, indeed, defective, so we are done. Figure 7b gives a non-defective picture $B_{3,2,2}$. Similarly, Figure 7c gives a non-defective picture $B_{4,2,2}$.

Now let $d \geq 5$ and write $d+1 = (3+1)q + (r+1)$ with $r \in \{1,3,4,6\}$. Then we can construct a non-defective picture $B_{d,2,2}$ from q copies of the non-defective picture $B_{3,2,2}$ and one non-defective picture $B_{r,2,2}$. This settles $B_{d,2,2}$.

For $B_{2,3,2}$ and $B_{1,3,2}$ we have already found non-defective pictures. For $d \geq 3$ write $d+1 = 2q + (r+1)$ with $r \in \{1,2\}$. Then one can construct a non-defective picture $B_{d,3,2}$ from q non-defective pictures $B_{1,3,2}$ and one non-defective picture $B_{r,3,2}$. This settles $B_{d,3,2}$.

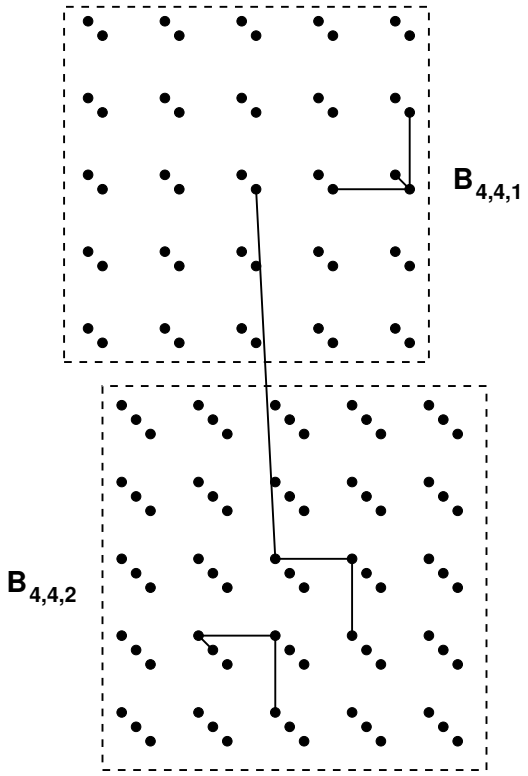

Figure 8: $B_{4,4,4}$.

If $d+1$ is even, then we can a construct non-defective picture $B_{d,e,2}$ with $d \geq e \geq 2$ as follows: write $e+1 = 2q+(r+1)$ with $r \in \{1,2\}$, and put together q non-defective pictures $B_{d,1,2}$ and one non-defective picture $B_{d,r,2}$.

Figure 7d shows how a copy of our earlier non-defective picture $B_{2,4,2}$ and a non-defective picture $B_{1,4,2}$ can be put together to a non-defective picture $B_{4,4,2}$. Now let $d \geq 6$ be even and write $d+1 = 4q+(r+1)$ with $r \in \{2,4\}$. Then one can construct a non-defective picture $B_{d,4,2}$ from q copies of our non-defective picture $B_{3,4,2}$ and one non-defective picture $B_{r,4,2}$. This settles $B_{d,4,2}$.

Now suppose that $d \geq e \geq 5$ and $f = 2$. Write $e+1 = 4 * q+(r+1)$ with $r \in \{1,2,3,4\}$. Then we can construct a non-defective picture $B_{d,e,2}$ from q non-defective pictures $B_{d,3,2}$ and one non-defective picture $B_{d,r,2}$. This concludes the case where $d \geq e \geq f = 2$.

Consider the case where $d \geq e \geq f = 3$. This case is easy now: write, for instance, $e+1 = q*2+(r+1)$ with $r \in \{1,2\}$. Then a non-defective picture $B_{d,e,3}$ can be constructed from q non-defective pictures $B_{d,1,3}$ and one non-defective picture $B_{d,r,3}$.

The above gives (by rotating) non-defective pictures $B_{d,e,4}$ for all $d \geq 1$ and $e \in \{1,2,3\}$. Figure 8 shows how to construct a non-defective picture $B_{4,4,4}$. It may need a

bit of explanation: the upper half is the non-defective picture $B_{4,4,1}$, of Figure 6c, except that the redundant two vertices have been separated. The lower half is the non-defective picture $B_{4,4,2}$ of Figure 7d. By joining the lower one of the superfluous vertices in the upper half with the triangle in the lower half, we create a non-defective picture $B_{4,4,4}$. The newly created snake does not threaten any building block, as the picture shows, nor are the heads of this snake threatened by other snakes. Now suppose that $d \geq e \geq 5$ and write $e+1 = 4q + (r+1)$ with $r \in \{1,2,3,4\}$. Then we find a non-defective picture $B_{d,e,4}$ from q non-defective pictures $B_{d,3,4}$ and one non-defective picture $B_{d,r,4}$.

Finally, suppose that $d \geq e \geq f \geq 5$, and write $f+1 = 4q + (r+1)$ with $r \in \{1,2,3,4\}$. Then a non-defective picture $B_{d,e,f}$ can be assembled from q non-defective pictures $B_{d,e,3}$ and one non-defective picture $B_{d,e,r}$. This concludes the proof of Theorem 1.3.

6 Secant dimensions of $\mathbb{P}^2 \times \mathbb{P}^1$

For Theorem 1.3 we first deal with the defective cases: the Segre–Veronese embeddings of degree $(2, \text{even})$ are all defective by [7, Example 3.2]. That the embedding of degree $(3,1)$ is defective can be proved using a polynomial interpolation argument, used in [5] for proving defectiveness of other secant varieties: Split $(3,1) = (2,0) + (1,1)$. Now it is easy to see that given 5 general points there exist non-zero forms f_1, f_2 of multi-degrees $(2,0)$ and $(1,1)$, respectively, that vanish on those points. But then the product $f_1 f_2$ vanishes on those points together with all its first-order derivatives; hence the 5-th secant variety does not fill the space. The proof below shows that its codimension is not more than 1.

For the non-defective proofs we have to solve the optimisation problems $\mathrm{AP}(B,k)$, where

$$B = \{(x,y,z) \in \mathbb{Z}^3 \mid x,y,z \geq 0, x+y \leq d, \text{ and } z \leq e\}.$$

We shall do a double induction over the degrees e and d: First, in Subsections 6.1–6.4 we treat the cases where e is fixed to $1,2,3,4$, respectively, by induction over d. Then, in Subsection 6.5 we perform the induction over e. We shall always think of the x-axis as pointing towards the reader, the y-axis as pointing to the right and the z-axis as the vertical axis. The picture for (d,e) will be denoted by $T_{d,e}$. We shall also use (non-defective) pictures $B_{a,b,c}$ from Section 5 as building blocks.

6.1 The cases where $e = 1$. Figures 9a–9d give pictures for $(d,1)$ with $d = 1,\ldots,4$. Now we explain how to construct a non-defective picture for $(d+4,1)$ from a non-defective picture for $(d,1)$. First translate $T_{d,1}$ four steps in the positive x-direction, and then proceed as follows.

(1) If $d+1$ is even, $d+1 = 2l$ for some l, then put l copies of $B_{1,3,1}$ to the left of $T_{d,1}$, starting at the origin. Finally, add a copy of $T_{2,1}$.
(2) If $d+1$ is odd, $d+1 = 2l+1$ for some l, then put one copy of $B_{2,3,1}$ and $l-1$ copies of $B_{1,3,1}$ to the left of $T_{d,1}$. Finally, add another copy of $T_{2,1}$.

This is illustrated in Figure 10.

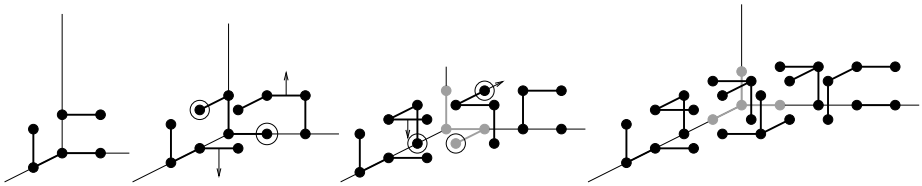

(a) $T_{1,1}$ (b) $T_{2,1}$ (c) $T_{3,1}$; defective (d) $T_{4,1}$

Figure 9: Induction basis for $(*, 1)$

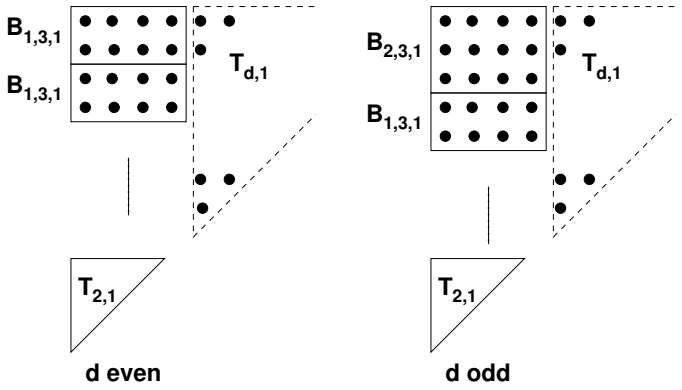

Figure 10: Induction step for $(*, 1)$

To complete the induction, since $T_{3,1}$ is defective, we need a non-defective picture for $(7, 1)$. We can construct this from two copies of $T_{2,1}$, one $B_{1,3,1}$ and one $B_{2,2,1}$ (at the origin) from Figure 5d. The remaining vertices are grouped together as in Figure 11 below. Note that one can separate the building blocks in this figure by successive planar cuts, so that Lemma 2.2 applies.

6.2 The cases where $e = 2$. Figures 12a–12i lay the basis for the induction over d. Note that $T_{6,2}$ is the first among the pictures whose number of vertices is divisible by 4. To finish the induction, we need to construct a non-defective picture for $(d + 8, 2)$ from $T_{d,2}$. First of all, move $T_{d,2}$ eight positions to the right. Then proceed as follows:

(1) If d is odd, $d = 2l+1$ for some $l \geq 0$, put l pairs of $B_{1,3,2}$ to the right of $T_{d,2}$ (starting at the origin), then two copies of $B_{2,3,2}$, and finally a copy of $T_{6,2}$.
(2) If d is even, $d = 2l$ for some $l > 0$, put $l + 1$ pairs of $B_{1,3,2}$ starting at the origin. Finish off with one copy of $T_{6,2}$.

This is illustrated in Figure 13.

6.3 The cases where $e = 3$. Here the induction over d is easier since every $T_{d,3}$ has its number of vertices divisible by 4. Figures 14a and 14b lay the basis of the induction

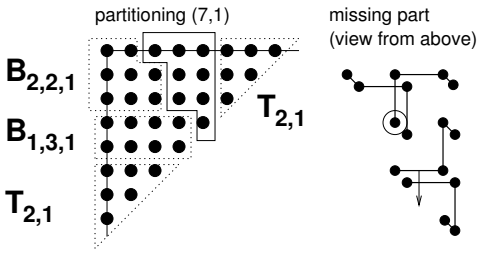

Figure 11: Obtaining $T_{7,1}$

(the latter just consists of two copies of $T_{2,1}$). Now we show that from a non-defective $T_{d,3}$ with d odd one can construct non-defective $T_{d+2,3}$ and $T_{d+3,3}$. Write $d = 2l + 1$, and proceed as follows.

(1) Move $T_{2l+1,3}$ two positions to the right. Put a block $B_{2l+1,1,3}$ at the origin, and conclude with a copy of $T_{1,3}$. This gives $T_{2l+3,3}$.
(2) Move $T_{2l+1,3}$ three steps to the right. Put a block $B_{2l+1,2,3}$ at the origin, and conclude with a copy of $T_{2,3}$.

For $d = 3$ this is illustrated in Figure 15.

6.4 The cases where $e = 4$. We proceed by induction. The induction step is identical to that for $e = 2$, except that the blocks $B_{1,3,2}$ and $B_{2,3,2}$ have to be replaced by the blocks $B_{1,3,4}$ and $B_{2,3,4}$, and $T_{6,2}$ has to be replaced by $T_{6,4}$. To lay the basis for the induction we need pictures for $d = 1, 2, 3, 4, 5, 6, 7, 8, 10$, where the last one is needed since $(2, 4)$ is defective. If $(d + 1)(d + 2)$, which is the number of points in $T_{d,1}$, is a multiple of 4 and both $T_{d,1}$ and $T_{d,2}$ are non-defective, then a non-defective $T_{d,4}$ is obtained by stacking $T_{d,1}$ on top of $T_{d,2}$. This is the case for $d = 6, 7, 10$. The same construction for $d = 2$ leads to a defective picture $T_{2,4}$, which shows that the defects are not worse than Theorem 1.3 claims. Hence only pictures $T_{d,4}$ for $d = 1, 3, 4, 5, 8$ are needed, and these are in Figures 16a–16e.

6.5 Induction over e. From a non-defective picture for (d, e) we can construct a non-defective picture for $(d, e + 4)$ by stacking a non-defective picture for $(d, 3)$, whose number of vertices is divisible by 4, on top of it. This settles all (d, e) except for those that are modulo $(0, 4)$ equal to the defective $(3, 1)$ or $(2, 2)$. The latter are easily handled, though: stacking copies of $T_{2,1}$ on top of $T_{2,2}$ gives pictures for all $(2, e)$ with e even that are defective but give the correct, known, secant dimensions. So to finish our proof of Theorem 1.3 we only need the non-defective picture for $(3, 5)$ of Figure 17.

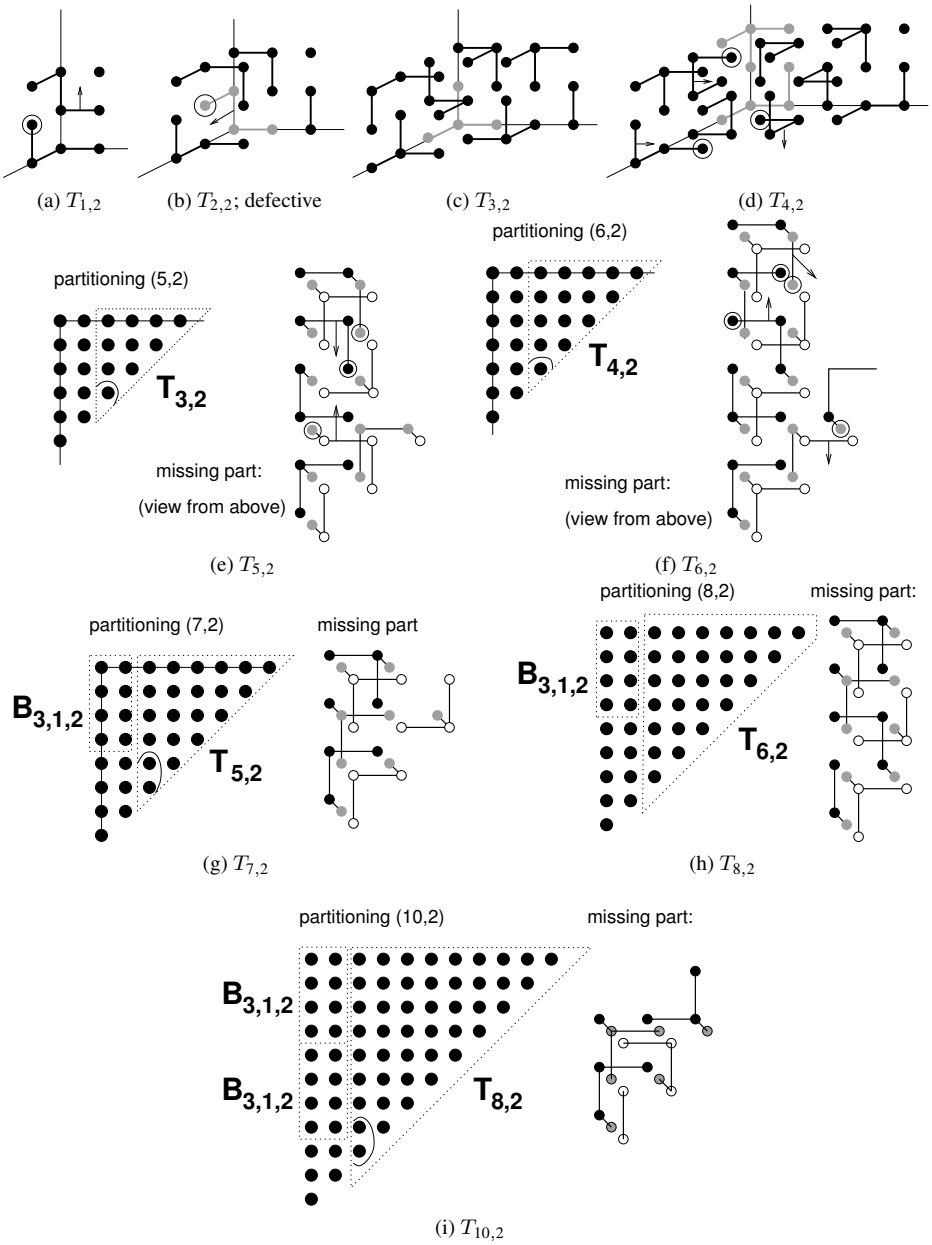

(a) $T_{1,2}$ (b) $T_{2,2}$; defective (c) $T_{3,2}$ (d) $T_{4,2}$

(e) $T_{5,2}$ (f) $T_{6,2}$

(g) $T_{7,2}$ (h) $T_{8,2}$

(i) $T_{10,2}$

Figure 12: Induction basis for $(*, 2)$.

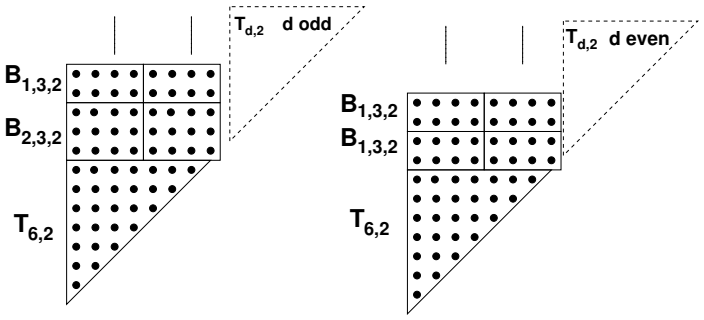

Figure 13: Induction step for $(*, 2)$

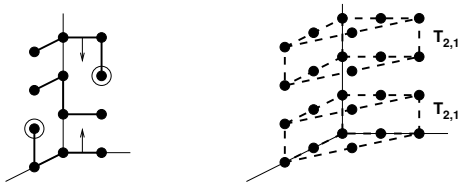

(a) $T_{1,3}$ (b) $T_{2,3}$

Figure 14: Induction basis for $(*, 3)$

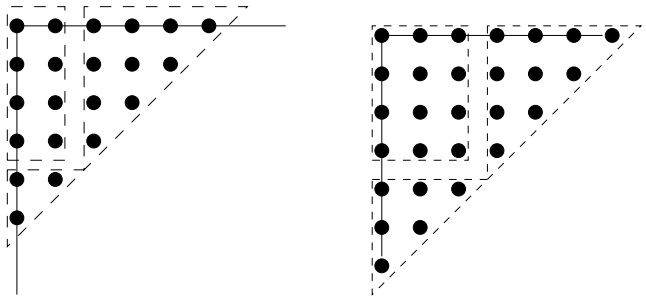

(a) odd $d + 2$ (b) even $d + 3$

Figure 15: Induction steps from $T_{3,3}$

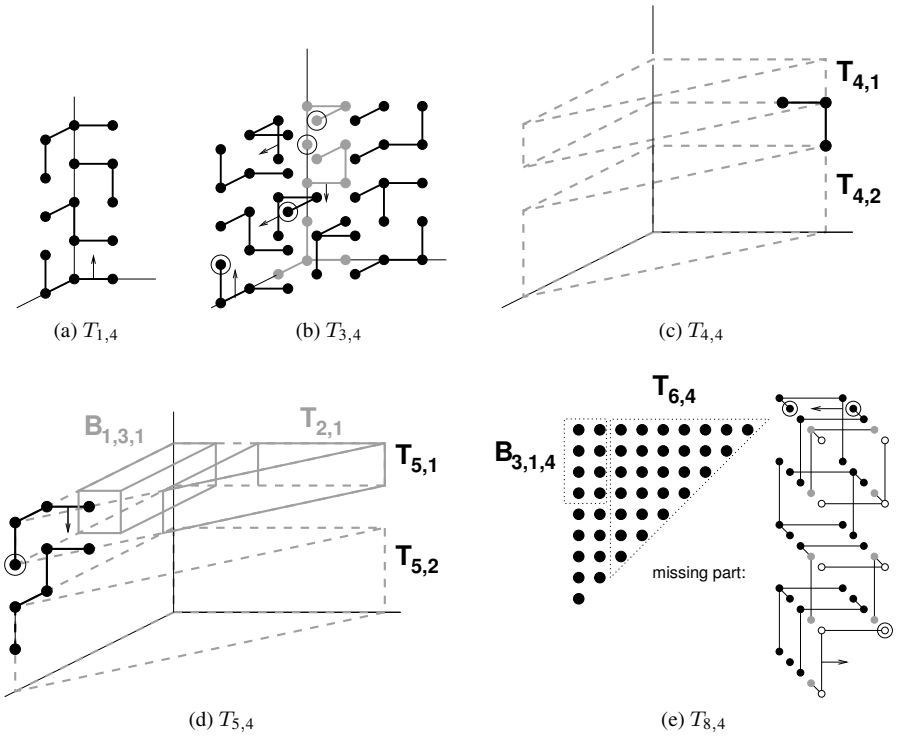

(a) $T_{1,4}$ (b) $T_{3,4}$ (c) $T_{4,4}$

(d) $T_{5,4}$ (e) $T_{8,4}$

Figure 16: Induction basis for $(*, 4)$

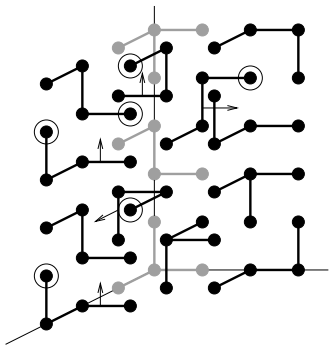

Figure 17: $T_{3,5}$

7 Secant dimensions of the point-line flag variety $\mathcal{F}$

In this section, $X = \mathcal{F}$, $G = \mathrm{SL}_3$, and the highest weight λ equals $m\omega_1 + n\omega_2$ with $m, n > 0$.

Remark 7.1. For the geometrically inclined reader we recall that the SL_3-equivariant embedding of $\mathcal{F}$ corresponding to highest weight λ is the one corresponding to the line bundle $\mathrm{SL}_3 /B \times_B K_{-\lambda} \to \mathrm{SL}_3 /B = X$ where B is the Borel subgroup and $K_{-\lambda}$ is the one-dimensional representation of B on which the torus $T \subseteq B$ acts with weight $-\lambda$. The global sections of this line bundle form an irreducible SL_3-module of highest weight λ by the Borel–Weil–Bott theorem. Below we shall point out a basis of this module consisting of PBW-monomials, which are in particular T-weight vectors. Unlike in the situation for Segre–Veronese embeddings, the T-weight spaces are not one-dimensional here, and we shall choose, in each weight space, PBW-monomials that are "small" in a suitable sense.

We first argue that $(m, n) = (1, 1)$ and $(m, n) = (2, 2)$ yield defective embeddings of $\mathcal{F}$. The first weight is the adjoint weight, so the cone $C_{1,1}$ over the image of $\mathcal{F}$ is just the set of rank-one, trace-zero matrices in $\mathfrak{sl}_3$, whose secant dimensions are well known. For the second weight let $C_{2,2}$ be the image of $C_{1,1}$ under the map $\mathfrak{sl}_3 \to S^2(\mathfrak{sl}_3), v \mapsto v^2$. Then $C_{2,2}$ spans the SL_3-submodule (of codimension 9) in $S^2(\mathfrak{sl}_3)$ of highest weight $2\omega_1 + 2\omega_2$, while it is contained in the quadratic Veronese embedding of $\mathfrak{sl}_3$. Viewing the elements of $S^2(\mathfrak{sl}_3)$ as symmetric 8×8-matrices, we find that $C_{2,2}$ consists of rank 1 matrices, while it is not hard to prove that the module it spans contains matrices of full rank 8. Hence $7C_{2,2}$ cannot fill the space.

For the non-defective proofs let α_1, α_2 be the simple positive roots, so that $X(\mathfrak{u}) = \{\beta_1, \beta_2, \beta_3\}$ with $\beta_1 = -\alpha_1$, $\beta_2 = -\alpha_1 - \alpha_2$ and $\beta_3 = -\alpha_2$. The subscripts indicate the order in which the PBW-monomials are computed: for $r = (n_1, n_2, n_3)$ we write $m_r := X_{\beta_1}^{n_1} X_{\beta_2}^{n_2} X_{\beta_3}^{n_3} v_\lambda$. Set

$$B := \{(n_1, n_2, n_3) \in \mathbb{Z}^3 \mid 0 \leq n_2 \leq m, 0 \leq n_3 \leq n, \text{ and } 0 \leq n_1 \leq m + n_3 - n_2\},$$

and let M be the set of all $r \in \mathbb{N}^{X(\mathfrak{u})}$ with $m_r \neq 0$. We shall not need M explicitly; it suffices to observe that $r_3 \leq n$ for all $r \in M$: indeed, if $r_3 > n$ then $X_{\beta_3}^{r_3} v_\lambda$ is already 0, hence so is m_r. We use the following consequence of the theory of canonical bases; see [8, Example 10, Lemma 11].

Lemma 7.2. *The m_b, $b \in B$, form a basis of V.*

Remark 7.3. The map $(n_1, n_2, n_3) \mapsto (n_1, n - n_3, m - n_2)$ sends the set B, which corresponds on the highest weight (m, n), to the set corresponding to the highest weight (n, m). Hence if we have a non-defective picture for one, then we also have a non-defective picture for the other. We shall use this fact occasionally.

We want to apply Lemma 2.6. First note that $r, r' \in \mathbb{R}^{X(\mathfrak{u})} = \mathbb{R}^3$ have the same weight if and only if $r - r'$ is a scalar multiple of $z := (1, -1, 1)$. We set $r < r'$ if and only if $r - r'$ is a *positive* scalar multiple of z.

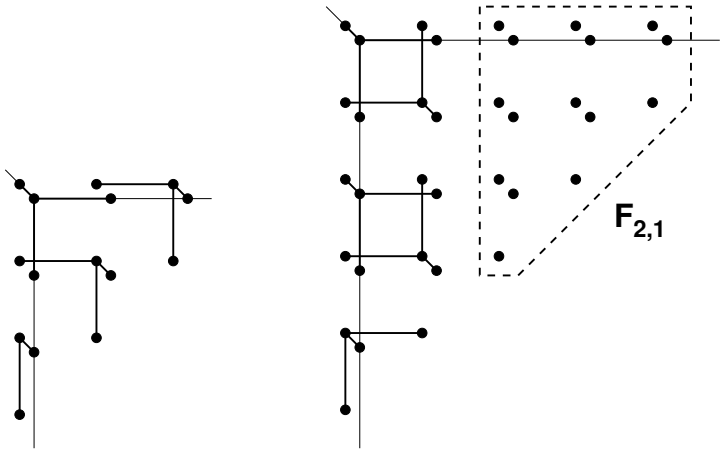

(a) $F_{2,1}$ (b) $F_{2+2k,1}$

Figure 18: Pictures $F_{\text{even},1}$.

Lemma 7.4. *For all $r \in M \setminus B$ and all $b \in B$ with $\xi(b) = \xi(r)$ we have $b < r$, i.e., the difference $b - r$ is a positive scalar multiple of z.*

Proof. Suppose that $b = (n_1, n_2, n_3) \in B$ and that $n_3 < n$. Then the defining inequalities of B show that $b + z = (n_1 + 1, n_2 - 1, n_3 + 1)$ also lies in B. This shows that B is a *lower ideal* in $(M, \leq)$, i.e., if $b \in B$ and $r \in M$ with $r < b$, then also $r \in B$. This readily implies the lemma. □

Proposition 7.5. $\mathrm{AP}^*(B, k)$ *is a lower bound on* $\dim kC$ *for all* k.

Proof. This follows immediately from Lemma 2.6 and Lemma 7.4 when we take for Z the one-dimensional cone $\mathbb{R}_{\geq 0} \cdot z$. □

In what follows we denote the picture for (m, n) by $F_{m,n}$, and we shall assume that $m \geq n$ when convenient. We first prove, by induction over m, non-defectiveness for $(m, 1)$ and $(m, 2)$, and then do induction over n to conclude the proof. Figure 19a for $(m, n) = (1, 1)$ is *not* non-defective, reflecting that the adjoint minimal orbit — the cone over which is the cone of 3×3-matrices with trace 0 and rank ≤ 1 — is defective. Figure 18a, however, shows a non-defective picture $F_{2,1}$, and from this picture one can construct non-defective pictures $F_{2+2k,1}$ by putting it to the right of k pictures, each of which consists of cubes and a single corner; Figure 18b illustrates this for the step from $F_{2,1}$ to $F_{2+2,1}$.

Figure 19b shows a non-defective picture for $F_{3,1}$, and Figure 19c a non-defective picture $F_{5,1}$. From these we can construct non-defective pictures $F_{3+4k,1}$ and $F_{5+4k,1}$, respectively, by putting them to the right of k pictures, each of which consists of a few cubes plus a non-defective picture for $F_{3,1}$ — Figure 19d illustrates this for the step from $F_{3,1}$ to $F_{7,1}$. This settles $F_{n,1}$.

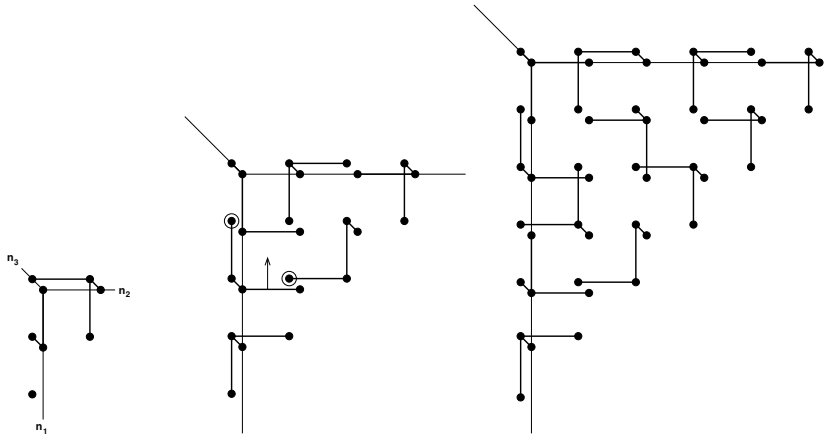

(a) $F_{1,1}$; defective (b) $F_{3,1}$ (c) $F_{5,1}$

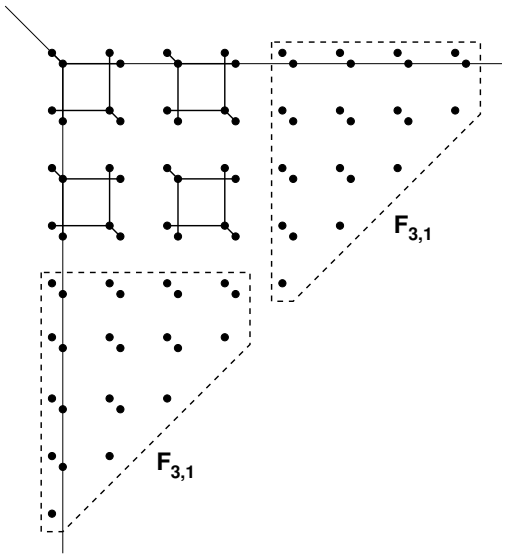

(d) $F_{3+4k,1}$

Figure 19: Pictures $F_{\text{odd},1}$

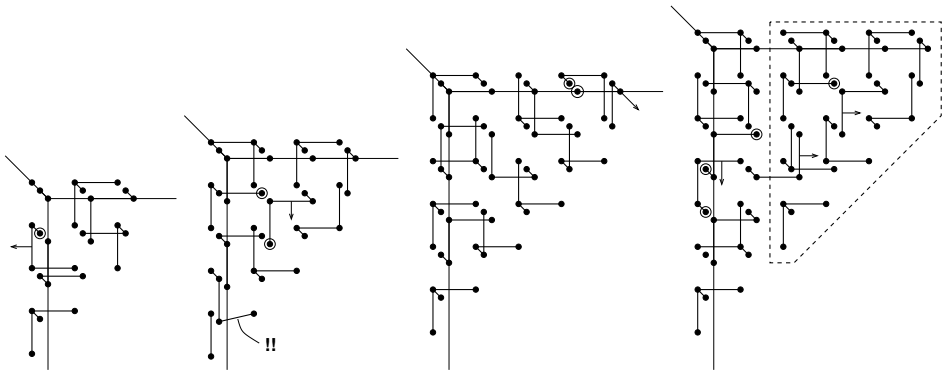

(a) $F_{2,2}$; defective (b) $F_{3,2}$ (c) $F_{4,2}$ (d) $F_{5,2}$

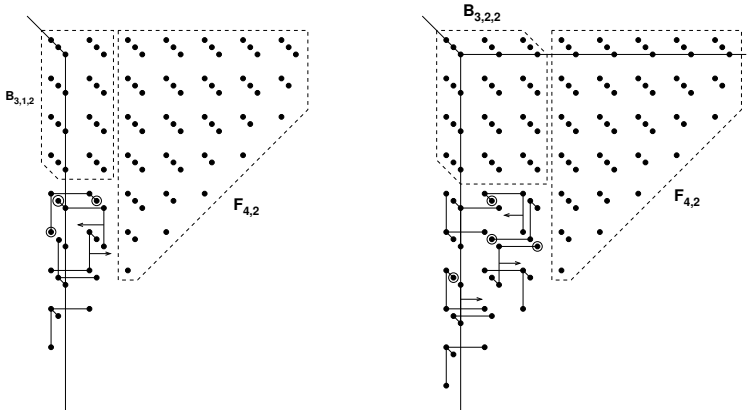

(e) $F_{6,2}$ (f) $F_{7,2}$

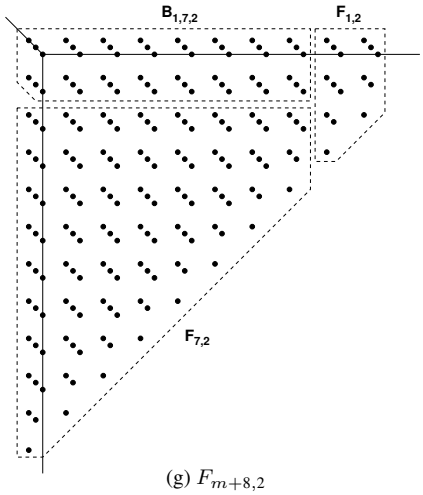

(g) $F_{m+8,2}$

Figure 20: Pictures $F_{*,2}$

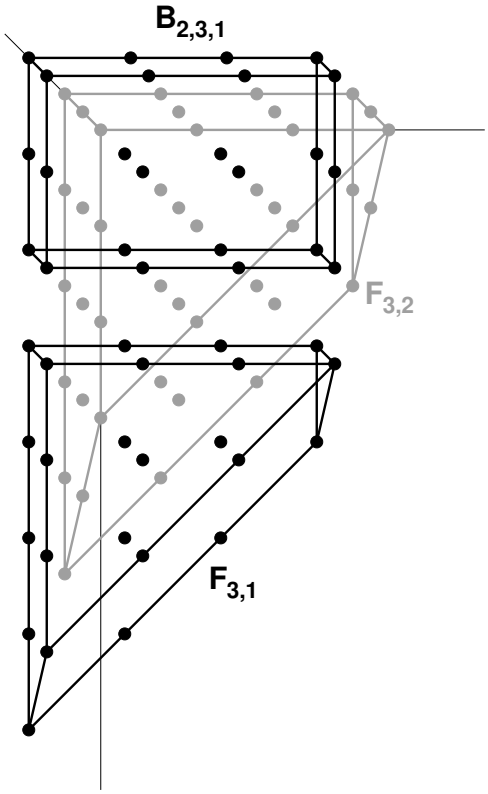

Figure 21: Construction for m or n odd.

Figure 20a is defective: it reflects the fact that the 7-th secant variety of X in the $F_{2,2}$-embedding has defect 1. Figure 20b gives a non-defective picture $F_{3,2}$. Note that one non-standard cells B_i is used here; this is because we want to line up the single edge with a single vertex in the construction of $F_{6,6}$. The non-standard block and the edge can be cut of from the rest by a planar cut, so that Lemma 2.2 yields non-defectiveness of $F_{3,2}$. Figure 20c gives a non-defective picture $F_{4,2}$. Figures 20d, 20e, and 20f give non-defective $F_{5,2}, F_{6,2}, F_{7,2}$. Similarly, one can construct pictures $F_{8,2}$ and $F_{10,2}$ — which are left out here because they take too much space. Finally, from a non-defective picture $F_{m,2}$ (with $m = 1$ or $m \geq 3$) one can construct a non-defective picture $F_{m+8,2}$ by inserting an $F_{7,2}$ and a block $B_{m,7,2}$ in front — Figure 20g illustrates this for $m = 1$. This settles the cases where $m \geq n = 2$.

Now all cases where at least one of m and n is odd can also be settled. Indeed, suppose that $m, n \geq 3$ and that m is odd. Write $n + 1 = 2q + (r + 1)$ with $r \in \{1, 2\}$. Then we can construct a non-defective picture $F_{m,n}$ by taking our non-defective picture $F_{m,r}$ and successively stacking q non-defective pictures of two layers on top, each of which pictures with a number of vertices divisible by 4. These layers can be constructed as

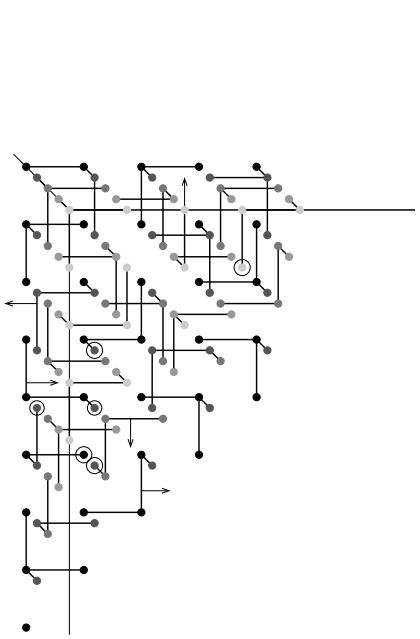

(a) $F_{4,4}$

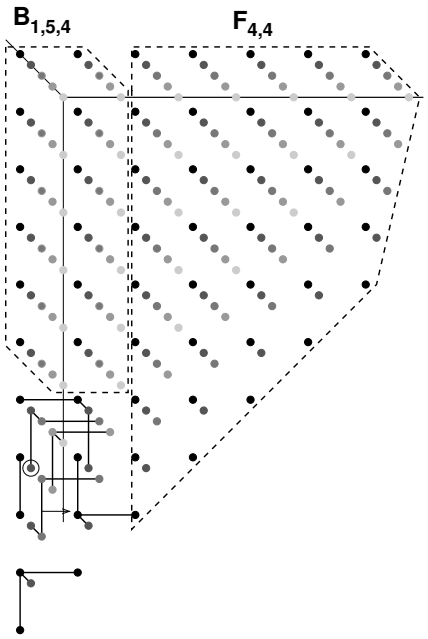

(b) $F_{6,4}$

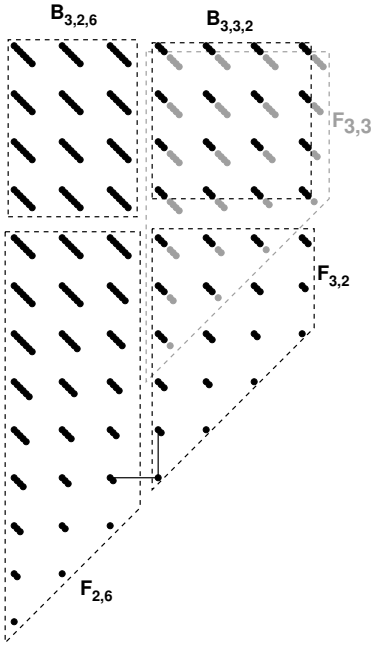

(c) $F_{6,6}$

Figure 22: Remaining base cases for the induction.

follows: the i-th layer consists of a block $B_{r+2i-2,m,1}$ (lying against the (n_2, n_3)-plane) and a non-defective picture $F_{m,1}$. As m is odd, each of these two blocks has a number of vertices divisible by 4. This construction is illustrated for $m = 3$ and $n = 4$ in Figure 21, where one extra layer is put on top of the "ground layer".

Only the cases remain where m and n are both even. We first argue that we can now reduce the discussion to a finite problem: if $m \geq 7$ and $n \geq 2$, then we can compose a non-defective picture $F_{m,n}$ from one non-defective picture $F_{7,n}$ (which exists by the above), one non-defective block $B_{7,m-8,n}$ (both of these have numbers of vertices divisible by 4), and one non-defective picture $F_{m-8,n}$ — if such a picture exists. Hence we may assume that $m < 7$. Similarly, by using Remark 7.3 we may assume that $n < 7$. Using that m, n are even, and that $m, n > 2$ (which we have already dealt with), we find that only $(4, 4)$, $(4, 6)$ (or $(6, 4)$), and $(6, 6)$ need to be settled — as done in Figures 22a–22c. The picture $F_{6,6}$ is built from a block $B_{3,2,6}$, one $F_{2,6}$ obtained from $F_{6,2}$, and one $F_{3,6}$; the latter picture, in turn, can be constructed as outlined above, except that, in order to line up the single edge in $F_{3,6}$ and the single vertex in $F_{2,6}$, the order of the building blocks for $F_{3,6}$ is altered: $F_{3,2}$ comes on top, next to a block $B_{3,3,2}$, and under these a copy of $F_{3,3}$. This is where we use that in $F_{3,2}$ the remaining two vertices form an edge in a convenient position, this explains the use of the non-standard building block for $F_{3,2}$. It is easy to see that the left-hand side of the picture, together with the single edge of $F_{3,2}$ in the right-hand side, can be separated from the rest with a plane, so that Lemma 2.2 yields non-defectiveness. This concludes the proof of Theorem 1.4.

References

[1] J. Alexander, A. Hirschowitz, Polynomial interpolation in several variables. *J. Algebraic Geom.* **4** (1995), 201–222. MR1311347 (96f:14065) Zbl 0829.14002

[2] A. Borel, *Linear algebraic groups*. Springer 1991. MR1102012 (92d:20001) Zbl 0726.20030

[3] M. C. Brambilla, G. Ottaviani, On the Alexander-Hirschowitz theorem. *J. Pure Appl. Algebra* **212** (2008), 1229–1251. MR2387598 (2008m:14104) Zbl 1139.14007

[4] S. Brannetti, Degenerazioni di Varietà Toriche e Interpolazione Polinomiale. PhD thesis, Università di Roma "Tor Vergata", 2007.

[5] M. V. Catalisano, A. V. Geramita, A. Gimigliano, Higher secant varieties of Segre-Veronese varieties. In: *Projective varieties with unexpected properties*, 81–107, de Gruyter 2005. MR2202248 (2007k:14109a) Zbl 1102.14037

[6] M. V. Catalisano, A. V. Geramita, A. Gimigliano, Segre–Veronese embeddings of $\mathbb{P}^1 \times \mathbb{P}^1 \times \mathbb{P}^1$ and their secant varieties. *Collect. Math.* **58** (2007), 1–24. MR2310544 (2008f:14069) Zbl 1122.14037

[7] M. V. Catalisano, A. V. Geramita, A. Gimigliano, On the ideals of secant varieties to certain rational varieties. *J. Algebra* **319** (2008), 1913–1931. MR2392585 (2009g:14068) Zbl 1142.14035

[8] W. A. de Graaf, Five constructions of representations of quantum groups. *Note Mat.* **22** (2003/04), 27–48. MR2106571 (2005i:17018) Zbl 1097.17013

[9] M. Develin, Tropical secant varieties of linear spaces. *Discrete Comput. Geom.* **35** (2006), 117–129. MR2183492 (2006g:52024) Zbl 1095.52006

[10] J. Draisma, A tropical approach to secant dimensions. *J. Pure Appl. Algebra* **212** (2008), 349–363. MR2357337 (2008j:14102) Zbl 1126.14059

[11] J. Harris, *Algebraic geometry*. Springer 1992. MR1182558 (93j:14001) Zbl 0779.14001

[12] J. E. Humphreys, *Introduction to Lie algebras and representation theory*. Springer 1972. MR0323842 (48 #2197) Zbl 0254.17004

[13] B. Sturmfels, S. Sullivant, Combinatorial secant varieties. *Pure Appl. Math. Q.* **2** (2006), 867–891. MR2252121 (2007h:14082) Zbl 1107.14045

Received 19 July, 2007; revised 9 February, 2009

K. Baur, ETH Zürich, Departement Mathematik, Rämistrasse 101, 8092 Zürich, Schweiz
Email: baur@math.ethz.ch

J. Draisma, Department of Mathematics and Computer Science, Technische Universiteit Eindhoven, P.O. Box 513, 5600 MB Eindhoven, The Netherlands, and Centrum voor Wiskunde en Informatica, Amsterdam, The Netherlands
Email: j.draisma@tue.nl